

## Characterization of Excel Alloy Pressure Tube Material for CANDU SCW Reactors

M. Sattari, R.A. Holt and M.R. Daymond

Queen's University, Ontario, Canada

(sattari@me.queensu.ca)

### Summary

The phase transformation temperatures, aging response, and creep rupture strength of Zr alloy Excel (Zr- 3.5%Sn- 0.8%Nb- 0.8%Mo) pressure tube material were investigated. The  $\alpha \rightarrow \alpha+\beta$  and  $\alpha+\beta \rightarrow \beta$  transus temperatures were found to be in the range of 600-690 °C and 962-975 °C respectively. Precipitation hardening was observed in the microstructures water-quenched from high in the  $\alpha+\beta$  or  $\beta$  regions followed by aging at 400-500 °C for 1 hr. The results of creep-rupture experiments at 400 °C suggest that a fully martensitic and aged microstructure has better creep properties at high stress levels (>700 MPa) and a microstructure obtained by air-cooling from high in the  $\alpha+\beta$  region shows good creep properties at lower stresses (<560 MPa).

### 1. Introduction

The thermal efficiency of CANDU reactors can be increased by increasing the coolant temperature, for example in the conceptual design of the Generation IV Super Critical Water CANDU reactor (CANDU-SCWR) a thermal efficiency of up to 40% is achieved by increasing the coolant temperature from 300°C to 650°C, by using a re-entrant channel design requiring the pressure tube to operate at 400 °C [1][2]. This implies the need for higher creep resistant material for pressure tube than Zr-2.5Nb which is the current material in use. Excel alloy (Zr- 3.5%Sn- 0.8%Nb- 0.8%Mo), a dual-phase  $\alpha$ -hcp and  $\beta$ -bcc material, is a good candidate material for pressure tubes. It is known that Zr-Sn-Nb-Mo alloys have higher strength and creep resistance compared to other Zr alloys [3][4] mainly due to solid solution strengthening effect of Sn as well as the potential for age hardening in the  $\alpha+\beta$  quenched condition.

In order to understand the metallurgy of this alloy and improve its mechanical properties, it is important to know the transformation temperatures, i.e.  $\alpha \rightarrow \alpha+\beta$  and  $\alpha+\beta \rightarrow \beta$ . Metallography techniques as well as Differential Scanning Calorimetry (DSC) and resistivity measurements have been employed to study the transformation temperatures. Microstructural characterization has been done using optical and electron microscopy. Different heat treatments have been developed to study the aging response of this alloy and to improve its mechanical properties, particularly creep resistance which is investigated using accelerated stress-rupture experiments.

## 2. Results

### 2.1 Transformation Temperatures

The transformation temperatures were studied using quantitative metallography, Differential Scanning Calorimetry (DSC), and resistivity measurement techniques. The  $\alpha \rightarrow \alpha+\beta$ , i.e. the temperature at which the volume fraction of stabilized  $\beta$  starts to increase, and  $\alpha+\beta \rightarrow \beta$  transus temperatures were found to be in the range 600-690 °C and 962-975 °C respectively.

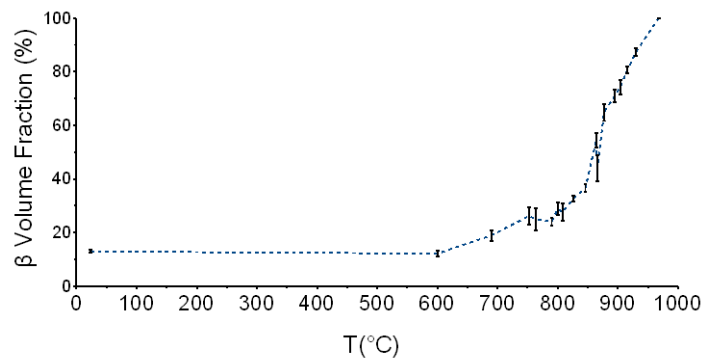


Figure 1 Volume fraction of beta-phase (%) as a function of temperature from which the samples were quenched. Error bars are determined according to the 95% confidence interval formula in ASTM E562-11.

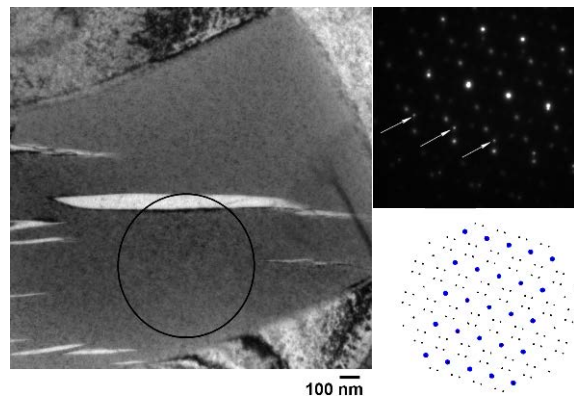


Figure 2 TEM micrograph and Selected Area Diffraction (SAD) pattern of sample water-quenched from 800°C. Bottom right is reconstruction of the  $\beta$ - and  $\omega$ -phase diffraction patterns.

For quantitative metallography quenching from different temperatures followed by metallography and Scanning Electron Microscopy (SEM) was used to study the transformation temperatures based on the microstructural changes. It is known that in  $\beta$ -stabilized Zr alloys, quenching from the  $\alpha+\beta$  or  $\beta$  region results in the transformation of  $\beta_{Zr}$  to  $\alpha'$ -hcp martensite,  $\alpha''$  orthorhombic martensite or  $\omega$  hexagonal metastable phases or a mixture of these depending on the solution

treatment temperature and chemical composition of the alloy. The  $\alpha'$ -hcp martensite appears in two morphologies: lath (massive) martensite in dilute alloys and acicular martensite, while the  $\omega$  phase is in the form of very fine (<0.5 nm) particles with no discernible shape [5][6]. Therefore, the occurrence of any of these metastable phases in the microstructure of the heated and quenched sample suggests the presence of the  $\beta$  phase prior to quenching. The result of quantitative metallography is shown in Figure 1 showing the change in the volume fraction of  $\beta$ -phase as a function of temperature.

$\beta$ -phase was observed to remain partially un-transformed upon quenching from temperatures below 860 °C; instead,  $\omega$ -phase and a few  $\alpha''$  martensite laths form inside the retained  $\beta$  (Figure 2). This is due to the fact that the amount of  $\beta$ -stabilizer elements, i.e. Mo, and Nb is high enough to prevent the martensitic transformation.

## 2.2 Aging Response

Studies on Zr-Mo, and Zr-Nb-Sn-Fe systems have shown the presence of intermetallic precipitates [7][8]. In this study aging response of Excel alloy was investigated through solution treatment of the alloy high in the  $\alpha+\beta$  and  $\beta$  regions followed by water-quenching and air-cooling and finally aging in the temperature range of 400-500 °C. Figure 3 shows the results in terms of hardness as a function of aging time. Transmission Electron Microscopy (TEM) showed the presence of very fine precipitates (5-10 nm) only in the martensitic phase (Figure 4). Energy Dispersive X-ray Spectroscopy (EDS) on the replica extracted precipitates of an over-aged sample showed the chemical composition to be Zr-30%Mo-25%Nb-2%Fe. Convergent Beam Electron Diffraction (CBED) and Selected Area Diffraction (SAD) ring patterns study on the precipitates, suggest that the crystal structure is hexagonal.

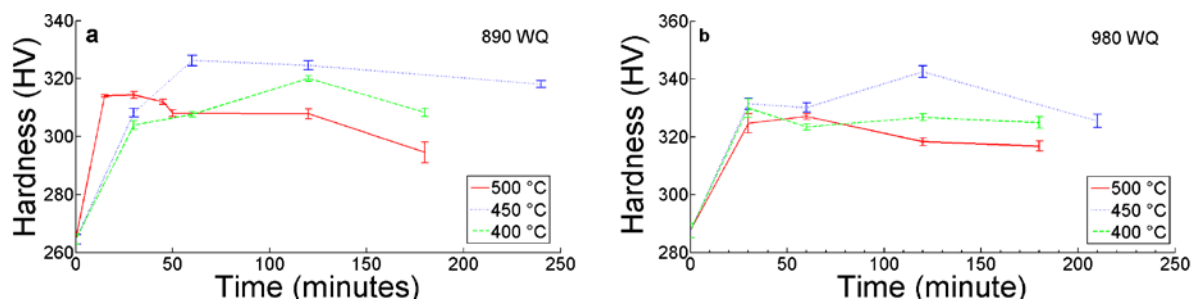


Figure 3 Hardness (HV) as a function of aging time for water-quenched from a) 890°C b) 980°C. (error bars are standard deviation obtained from at least 5 measurements).

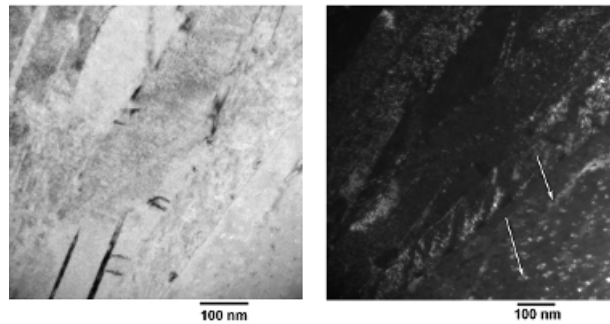


Figure 4 Multiple beam Bright Field (left) and Dark Field (right) TEM micrographs of the martensitic phase showing the precipitates.

### 2.3 Creep-Rupture

The creep-rupture strength of Excel alloy in the water-quenched and aged conditions as well as air-cooled condition was studied in the axial and transverse direction of pressure tube the result of which is presented in Figure 5.

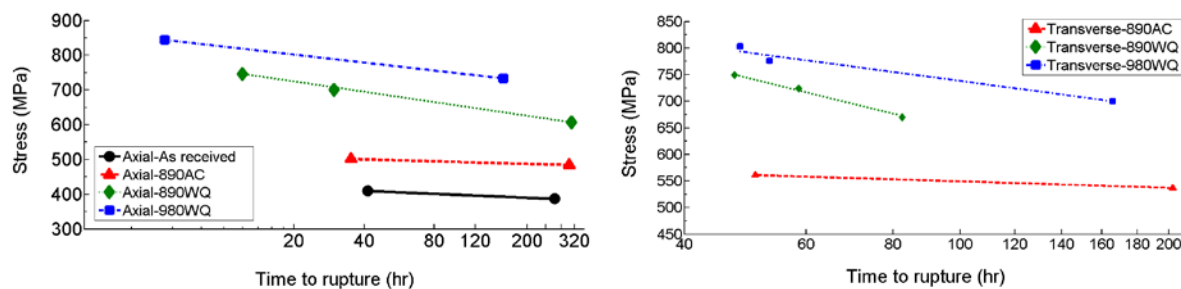


Figure 5 Creep-rupture graphs of different microstructures in the axial (left) and transverse (right) directions.

Texture of all the heat treated samples is more random compared to the typical pressure tube texture, which has most of the basal plane normal in the transverse direction of the tube. A more random texture will result in lower deformation anisotropy.

Steady state creep rates (Figure 6) show that the fully martensitic microstructure resulting from  $\beta$ -quenching and aging has very low creep rates despite the very high stress levels (>700 MPa) at which it was tested. At lower stress levels (<560 MPa) the microstructure obtained from air-cooling from high in the  $\alpha+\beta$  Widmanstätten (890AC) shows better creep resistance compared to the as-received annealed pressure tube material. Fractography on the creep-rupture samples showed dimple fracture surface typical of ductile failure for all the microstructures; however there was evidence of intergranular fracture for the  $\beta$ -quenched fully martensitic sample which is likely due to grain boundary segregation of impurity elements such as Cl and P which are known to have deleterious effects on fracture properties of Zr alloys [9].

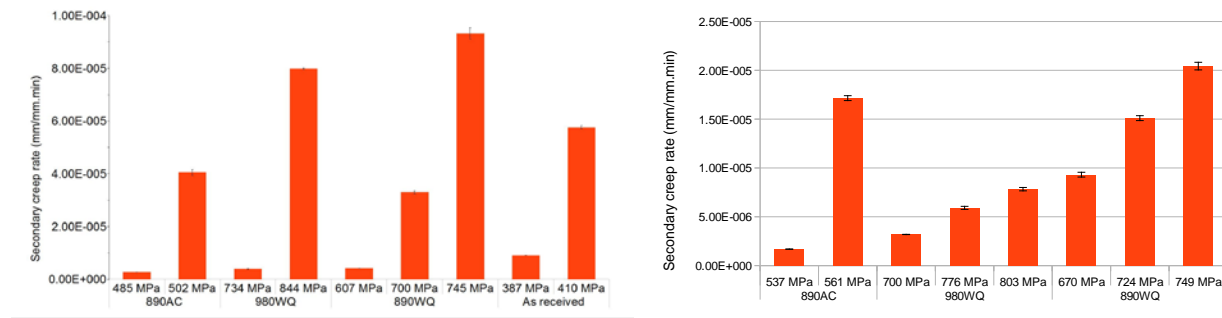


Figure 6 Steady-state creep rates of different microstructures tested in the axial (left) and transverse (right) directions.

### 3. References

- [1]. Chow C.K., Khartabil H.F., “Conceptual Fuel Channel Design for CANDU-SCWR”, *Nuclear Engineering and Technology*, Vol. 40, No. 2, 139-146.
- [2]. Torgerson D.F., Shalaby B.A., Pang S., “CANDU technology for Generation III+ and IV reactors”, *Nuclear Engineering and Design*, 236 (2006), 1565-1572.
- [3]. Cheadle B.A., Holt R.A., Fidleris V., Causey A.R., Urbanic V.F., “High Strength, Creep-Resistant Excel Pressure Tube”, *Zirconium in The Nuclear Industry*, STP 754 (1982), 193-207.
- [4]. Ibrahim E.F., Price E.G., Wysiekiersky A.G., “Creep and Stress-Rupture of High Strength Zirconium Alloys”, *Canadian Metallurgical Quarterly*, Vol. 11, No. 1 (1972), 273-283.
- [5]. Banerjee S., Mukhopadhyay P., “Phase Transformation: Titanium and Zirconium Alloys”, Elsevier Science, 1 edition (2007).
- [6]. Banerjee S., Krishnan R., “Martensitic Transformation in Zirconium-Niobium Alloys”, *Acta Metallurgica*, Vol. 19 (1971), 1317-1326.
- [7]. Zinkevich M., Mattern N., “Thermodynamic Assessment of the Mo-Zr System”, *Journal of Phase Equilibria*, Vol. 23, No. 2 (2002), 156-162.
- [8]. Toffolon C., Brachet J.C., Servant C., Legras L., Charquet D., Barberis P., Mardon J.P., “Experimental Study and Preliminary Thermodynamic Calculations of The Pseudo-Ternary Zr-Nb-Fe-(O,Sn) System”, *Zirconium in The Nuclear Industry*, 13th International Symposium, ASTM STP 1423, 361-382.
- [9]. Nikulina A. V., Malgin A. G., “Impurities and Their Effect on the Structure and Properties of Zirconium Parts in Nuclear Reactors”, *Atomic Energy*, Vol. 105, No. 5 (2008), 328-339.